

The peculiar Ca-rich SN 2019ehk: Evidence for a Type IIb core-collapse supernova from a low mass stripped progenitor

KISHALAY DE,¹ U. CHRISTOFFER FREMLING,¹ AVISHAY GAL-YAM,² MANSI M. KASLIWAL,¹ AND S. R. KULKARNI¹

¹*Cahill Center for Astrophysics, California Institute of Technology, 1200 E. California Blvd. Pasadena, CA 91125, USA*

²*Benoziyo Center for Astrophysics, The Weizmann Institute of Science, Rehovot 76100, Israel*

Submitted to ApJL

ABSTRACT

The nature of the peculiar ‘Ca-rich’ SN 2019ehk in the nearby galaxy M100 remains unclear. Its origin has been debated as either a stripped core-collapse supernova or a thermonuclear helium detonation event. Here, we present very late-time photometry of the transient obtained with the Keck I telescope at ≈ 280 days from peak light. Using the photometry to perform accurate flux calibration of a contemporaneous nebular phase spectrum, we measure an [O I] luminosity of $(0.23 - 0.78) \times 10^{38}$ erg s⁻¹ and [Ca II] luminosity of $(3.4 - 9.1) \times 10^{38}$ erg s⁻¹ over the range of the uncertain extinction along the line of sight. We use these measurements to derive lower limits on the synthesized oxygen mass of $\approx 0.005 - 0.05 M_{\odot}$. The oxygen mass is a sensitive tracer of the progenitor mass for core-collapse supernovae, and our estimate is consistent with explosions of very low mass CO cores of $1.45 - 1.5 M_{\odot}$, corresponding to He core masses of $\approx 1.8 - 2.0 M_{\odot}$. We present high quality peak light optical spectra of the transient and highlight features of hydrogen in both the early (‘flash’) and photospheric phase spectra, that suggest the presence of $\gtrsim 0.02 M_{\odot}$ of hydrogen in the progenitor at the time of explosion. The presence of H, together with the large [Ca II]/[O I] ratio ($\approx 10 - 15$) in the nebular phase is consistent with SN 2019ehk being a Type IIb core-collapse supernova from a stripped low mass ($\approx 9 - 9.5 M_{\odot}$) progenitor, similar to the Ca-rich SN IIb iPTF 15eqv. These results provide evidence for a likely class of ‘Ca-rich’ core-collapse supernovae from stripped low mass progenitors in star forming environments, distinct from the thermonuclear Ca-rich gap transients in old environments.

Keywords: supernovae: general — supernovae: individual (SN 2019ehk, iPTF 15eqv) — stars: massive — stars: mass-loss

1. INTRODUCTION

Ca-rich gap transients are an intriguing class of faint and fast evolving explosions characterized by their conspicuous strong [Ca II] $\lambda\lambda 7291, 7324$ emission (compared to [O I] $\lambda\lambda 6300, 6364$) in the nebular phase (Filippenko et al. 2003; Perets et al. 2010; Kasliwal et al. 2012; Valenti et al. 2014; Lunnan et al. 2017; Gal-Yam 2017; Milisavljevic et al. 2017; De et al. 2020). Tracking down the progenitors and explosion mechanisms of these unique transients is important for our understanding of the fates of close binary systems, the progenitors of Type

Ia SNe and the cosmic nucleosynthesis of Ca (Mulchaey et al. 2014; Frohmaier et al. 2019; De et al. 2020).

The peculiar SN 2019ehk was discovered in the galaxy M100 (Grzegorzek 2019), and subsequent follow-up showed that the source exhibited fast photometric and spectroscopic evolution to the nebular phase dominated by strong [Ca II] emission, consistent with several known properties of Ca-rich events (Jacobson-Galán et al. 2020; Nakaoka et al. 2020). Jacobson-Galán et al. (2020) suggested that its early fast spectroscopic evolution and double peaked light curve is likely explained with an explosive thermonuclear detonation ignited during a white dwarf merger involving a low mass hybrid white dwarf. However, archival Hubble Space Telescope (HST) images could not rule out a core-collapse explosion from a $< 10 M_{\odot}$ massive star. On the other hand, Nakaoka

et al. (2020) favored a scenario involving a low-mass core-collapse supernova (SN) from an inflated and ‘ultra-stripped’ He star in a close binary system (Tauris et al. 2013, 2015) – a channel which has been suggested to lead to the formation of neutron stars in compact binary systems. As one of the nearest potential members of the class of Ca-rich events, constraining the nature of the progenitor of SN 2019ehk can reveal important clues to the broader population of events.

With the advent of large systematic experiments for supernova (SN) classification, it is now well established that Ca-rich gap transients are relatively common ($\approx 15\%$ of the SN Ia rate) and predominantly occur in old environments in the outskirts of early type galaxies, suggesting progenitor systems likely involving explosive He shell burning on low mass white dwarfs (Perets et al. 2010; Kasliwal et al. 2012; Lunnan et al. 2017; Frohmaier et al. 2018; De et al. 2020). The dominance of cooling via [Ca II] emission as opposed to Fe emission (seen in normal Type Ia SNe) has been recently shown to be a hallmark feature of explosions involving shell detonations (Waldman et al. 2011; Dessart & Hillier 2015) with low total (core + shell) masses (Polin et al. 2019).

However, the discovery of Ca-rich SNe such as iPTF 15eqv (Milisavljevic et al. 2017) and iPTF 16hgs (De et al. 2018a) in actively star forming environments (as in the case of SN 2019ehk) have also led to suggestions involving core-collapse supernovae from low mass progenitors. Yet, the high [Ca II]/[O I] ratio seen in the population of Ca-rich transients (Valenti et al. 2014; Milisavljevic et al. 2017; De et al. 2020) is strikingly different from that seen in normal stripped core-collapse SNe (Fang et al. 2019).

Oxygen in the ejecta of core-collapse SNe is formed primarily in the hydrostatic burning phase of the progenitor (increasing with zero age main sequence mass), while Ca is explosively synthesized by O burning (Fransson & Chevalier 1989; Woosley & Heger 2007). As a result, the O mass in the ejecta and Ca/O ratio is a powerful tracer of the progenitor mass for core-collapse SNe (Fransson & Chevalier 1989; Jerkstrand et al. 2014, 2015). In the case of the Ca-rich SN 2005cz, Kawabata et al. (2010) thus first suggested that the high [Ca II]/[O I] ratio could be explained by an explosion of a low mass progenitor that was stripped by a binary companion.

In this paper, we attempt to constrain the progenitor of SN 2019ehk with new late-time photometry and high quality optical spectra obtained near peak light. Section 2 provides an overview of the observations and data analysis procedures. We use the observations to constrain the composition of the ejecta in both the

early photospheric and late nebular phase in Section 3. We present a discussion on the likely progenitor for SN 2019ehk in Section 4 and conclude with a summary in Section 5. We adopt a distance of 16.2 Mpc and redshift of $z = 0.005$ to M100 for the rest of this work (Folatelli et al. 2010).

2. OBSERVATIONS AND ANALYSIS

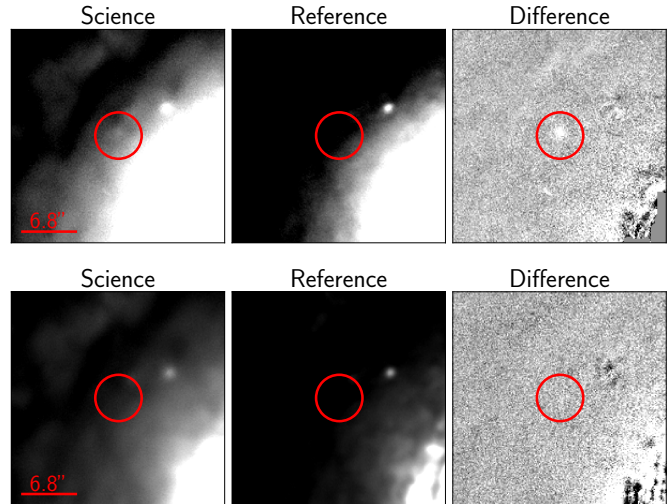


Figure 1. (Top panel) Late-time I -band detection of SN 2019ehk with the Keck-I telescope, with North up and East left. The left panel is the image taken at ≈ 280 days from peak light, the middle panel is the template image acquired at ≈ 400 days after peak light and the right panel is the difference image obtained after image subtraction. (Bottom panel) Same as top panel showing non-detection of SN 2019ehk at the same epoch in g band.

We obtained one epoch of late-time imaging of SN 2019ehk with the Low Resolution Imaging Spectrometer (LRIS; Oke et al. 1995) on the Keck-I telescope on UT 2020-02-18.62, at a phase of ≈ 280 days from r -band peak, for a total exposure time of 300s and 390s in g and I bands respectively. We obtained a reference epoch for the source on UT 2020-06-23.32 to use as a template for image subtraction of the host galaxy light, for a total exposure time of 520s and 440s in g and I bands respectively. The data were reduced using `lpipe` (Perley 2019) and image subtraction was performed using `HOTPANTS` (Becker 2015).

Photometric calibration was performed against SDSS catalog magnitudes of secondary standards in the field. The source is clearly detected in the I -band subtracted image at a magnitude of $I = 22.10 \pm 0.15$ AB mag (Figure 1), while the source is not detected in g -band to a 3σ depth of 23.55 AB mag. Based on the observed decay rate of the late-time light curve ($\gtrsim 0.02$ mag day $^{-1}$;

Jacobson-Galán et al. 2020), we expect the flux of the source at the template image epoch (≈ 400 days) to be $\gtrsim 10\times$ smaller than the science epoch, and thus not contaminate our measurements significantly.

We use the observed late-time photometry to calibrate the published late-time spectrum at ≈ 260 days in Jacobson-Galán et al. (2020), noting that the strong [Ca II] line falls completely within the observed I band. We perform spectrophotometric calibration by convolving the filter function with the observed spectrum, and then measure the resulting line fluxes by trapezoidal integration of the respective wavelength regions. Uncertainties in this method are estimated by Monte Carlo sampling of the estimated fluxes by adding noise (scaled to nearby regions with no line emission) to the line profile, and add it in quadrature to the uncertainty of the photometric measurement. We measure the resulting [Ca II] line flux to be $(4.0 \pm 0.6) \times 10^{-15}$ erg cm $^{-2}$ s $^{-1}$ and the corresponding observed [O I] line flux to be $(2.1 \pm 0.4) \times 10^{-16}$ erg cm $^{-2}$ s $^{-1}$.

We also present optical spectroscopy of the transient obtained with the Double Beam Spectrograph (DBSP; Oke & Gunn 1982) on the Palomar 200-inch telescope (P200) on UT 2019-05-13, corresponding to a phase of $\approx +0$ days from r -band peak. The DBSP data were reduced using the `pyraf-dbsp` pipeline (Bellm & Sesar 2016). The data presented here will be publicly released on WISERep (Yaron & Gal-Yam 2012).

3. RESULTS

3.1. Correcting for host galaxy extinction

There is evidence for significant host galaxy extinction towards SN 2019ehk (Jacobson-Galán et al. 2020; Nakaoka et al. 2020). A deep Na I D line is clearly detected in its peak light spectra, and suggest a large host extinction of $E(B - V) \gtrsim 1$ based on canonical relationships between $E(B - V)$ and the equivalent width (EW) of the Na D line (Poznanski et al. 2012). However, the very large equivalent width ($EW \approx 3 \text{ \AA}$) falls in a regime where published relationships become uncertain (Poznanski et al. 2012). The adopted extinction thus introduces a large uncertainty in the determination of the absolute luminosity of the supernova and the nebular phase spectral lines.

However, the double-peaked light curve of SN 2019ehk shares several similarities with previously reported fast evolving Type I SNe in the literature, including the SN Ic iPTF 14qqr (De et al. 2018b) as well as the SN Ib iPTF 16hgs (De et al. 2018a). Nakaoka et al. (2020) show that the photometric properties of SN 2019ehk can match either the low peak luminosity of iPTF 16hgs or the higher luminosity of iPTF 14qqr for assumed extinc-

tions of $E(B - V) = 0.5$ mag and $E(B - V) = 1.0$ mag respectively, with the true value being likely in between these two¹. Taking these two values of extinction as limiting cases, we obtain extinction corrected [O I] flux of $(7.2 \pm 1.3) \times 10^{-16}$ erg cm $^{-2}$ s $^{-1}$ and $(2.5 \pm 0.4) \times 10^{-15}$ erg cm $^{-2}$ s $^{-1}$ respectively assuming $R_V = 3.1$ and a Cardelli et al. (1989) extinction law. The corresponding [Ca II] line fluxes are $(1.1 \pm 0.2) \times 10^{-14}$ erg cm $^{-2}$ s $^{-1}$ and $(2.9 \pm 0.4) \times 10^{-14}$ erg cm $^{-2}$ s $^{-1}$.

3.2. Constraints on the oxygen mass

Uomoto (1986) provides an analytical formula to calculate the minimum O mass required for a given [O I] luminosity, which depends on the temperature of the emitting region. The relationship holds in the high density limit ($N_e \gtrsim 10^6$ cm $^{-3}$) where the electron density is above the [O I] critical density ($\sim 7 \times 10^5$ cm $^{-3}$), and is estimated to hold in this case for the estimated ejecta mass of $\approx 0.5 M_\odot$ (Jacobson-Galán et al. 2020; Nakaoka et al. 2020). However, we caution that such O mass estimates assume that the radioactive power deposited in the O-rich shells of the ejecta is released via cooling in the [O I] lines. Dessart & Hillier (2020) show that even small amounts of Ca mixing (~ 0.01 by mass fraction) from the underlying Si-rich layers can drastically reduce the [O I] line fluxes since [Ca II] is a much more effective coolant than [O I]. In the case of SN 2019ehk, it is clear that the majority of the cooling is arising from the [Ca II] line, which may be due to either a very low O layer mass compared to the Si-rich layer, or due to enhanced mixing of Ca into O-rich layers. As such, these O mass estimates should be treated as lower limits on the O mass in the ejecta.

While the temperature can be constrained with the line ratio of the [O I] $\lambda 5777 \text{ \AA}$ line to the [O I] $\lambda \lambda 6300, 6364$ doublet (Houck & Fransson 1996), the weak [O I] line in the SN 2019ehk spectrum at +260 days does not allow this measurement. Instead, we adopt a range of typical values estimated from the [O I] emission in other core-collapse SNe of $\approx 3400 - 4000$ K (Sollerman et al. 1998; Elmhamdi 2011). Taking the assumed distance to M100, we derive lower limits on the O mass in the range of $\approx 0.005 - 0.05 M_\odot$ over the range of temperature and extinctions. In particular, we note that the derived masses are typically one order of magnitude smaller than the inferred O masses in normal core-collapse SNe (Elmhamdi 2011; Jerkstrand et al. 2015; Dessart & Hillier 2020).

¹ The value of $E(B - V) = 0.47$ adopted in Jacobson-Galán et al. (2020) is at the lower limit of the range of extinction assumed here

The mass estimates derived here are inconsistent with that reported in [Jacobson-Galán et al. \(2020\)](#), who derive a much higher O mass of $\gtrsim 0.15 M_{\odot}$. This is likely because i) they derived these estimates using a spectrum at an earlier phase (≈ 60 days from peak) where the source was not completely nebular and ii) they assume that the Ca and O emitting regions are co-located in the ejecta so that the observed $[\text{Ca II}]/[\text{O I}]$ ratio directly constrains the Ca/O mass fraction and O mass via the $[\text{Ca II}]$ luminosity. However, we find this interpretation to be unlikely as detailed modeling of core-collapse SNe has shown that the $[\text{Ca II}]$ line serves as the primary coolant of the energy deposited in the Si-rich layers, while the $[\text{O I}]$ emission arises from the outer O-rich layers produced largely in the hydrostatic burning phase ([Jerkstrand et al. 2015](#); [Dessart & Hillier 2020](#)). Similar arguments for ejecta stratification also have been demonstrated with detailed modeling of thermonuclear shell detonations ([Dessart & Hillier 2015](#)).

3.3. Constraints on the progenitor mass

First, in order to directly compare the observed $[\text{O I}]$ luminosity with detailed nebular phase models of stripped envelope SNe and constrain the progenitor mass, we show in Figure 2, tracks of the $[\text{O I}]$ luminosity evolution for models of different initial ZAMS masses from [Jerkstrand et al. \(2015\)](#). As shown, the nebular models of relatively higher mass progenitors ($\approx 12 - 15 M_{\odot}$) from [Jerkstrand et al. \(2015\)](#) significantly overestimate the $[\text{O I}]$ luminosity, suggesting a much lower progenitor core mass for SN 2019ehk. Note that this conclusion is independent of the assumed extinction, since the $[\text{O I}]$ luminosity and the ^{56}Ni luminosity scale similarly with varying extinction.

Estimates of the O yields for such low progenitor (and CO core) masses are sparse in the literature, and have thus far been calculated for the case of the highly stripped He cores of ultra-stripped SNe ([Tauris et al. 2013](#)). In these scenarios, relatively low mass He stars ($\lesssim 3.5 M_{\odot}$) are stripped down to the CO core by a close binary companion, leaving behind low mass CO cores of $\approx 1.45 - 1.6 M_{\odot}$ at the time of explosion ([Tauris et al. 2015](#)). Although the presence of strong He lines in the spectra of SN 2019ehk suggests that the stripping did not extend down to the CO core, the nucleosynthetic O yields in these models are applicable to constrain the CO core mass at the time of explosion. Specifically, we note that the CO core mass is relatively insensitive to the mass loss processes via binary interactions that occur in the very late stages of stellar evolution ([Jerkstrand et al. 2015](#); [Podsiadlowski et al. 1992](#); [Woodsley & Heger 2015](#); [Laplace et al. 2020](#)), and hence a good tracer of

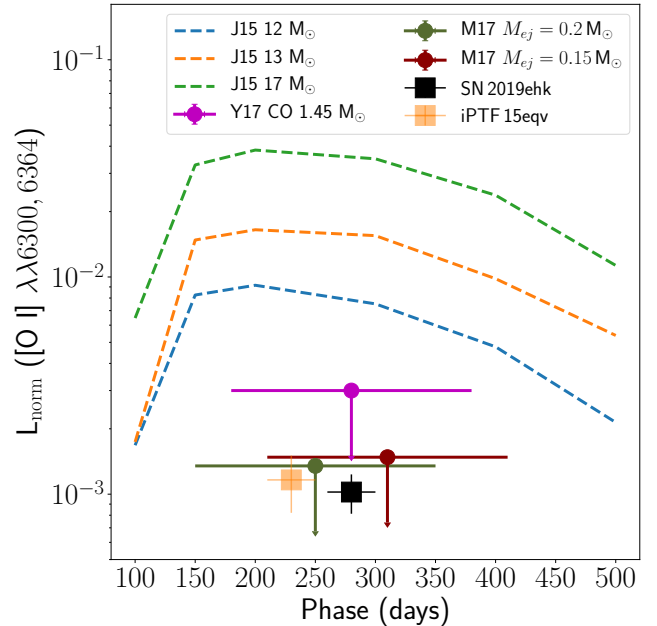


Figure 2. Comparison of the $[\text{O I}]$ luminosity of SN 2019ehk to models of stripped envelope core-collapse supernovae from [Jerkstrand et al. \(2015, J15\)](#). The $[\text{O I}]$ luminosity on the y-axis (denoted as L_{norm}) is normalized to the radioactive energy deposition rate from ^{56}Co decay, as done in [Jerkstrand et al. \(2015\)](#). In addition, we show estimated $[\text{O I}]$ luminosities from the nucleosynthesis calculations of [Moriya et al. \(2017, M17\)](#) for different ejecta masses from a $1.5 M_{\odot}$ CO core) and [Yoshida et al. \(2017, Y17\)](#), where we use the approximate relationship between $[\text{O I}]$ luminosity and oxygen mass in [Uomoto \(1986\)](#), assuming a temperature of 3400 K. The ultra-stripped model luminosity estimates have been arbitrarily shifted in phase for better visualization since the [Uomoto \(1986\)](#) estimate does not capture time evolution. For comparison, we also show the measured normalized $[\text{O I}]$ luminosity of another Ca-rich SNIb iPTF 15eqv.

the progenitor ZAMS mass ([Fransson & Chevalier 1989](#); [Jerkstrand et al. 2014, 2015](#)).

We use the nucleosynthetic yields from [Moriya et al. \(2017\)](#) and [Yoshida et al. \(2017\)](#) to estimate the $[\text{O I}]$ ([Uomoto 1986](#)) and ^{56}Ni luminosity in the nebular phase for low mass CO cores of $1.45 - 1.5 M_{\odot}$, under different assumptions of the explosion energy and ejecta mass. The $[\text{O I}]$ luminosity estimate assumes that all the synthesized O emits in $[\text{O I}]$ and hence serve as upper limits to the observed luminosity. Figure 2 shows that the upper limits on the $[\text{O I}]$ luminosity for the low mass CO core models are very similar to the low $[\text{O I}]$ luminosity measured for SN 2019ehk.

Next, we also use the derived O mass limits to constrain the progenitor ZAMS mass for SN 2019ehk. In Figure 3, we plot model tracks showing the steep dependence of synthesized O mass on the progenitor ZAMS

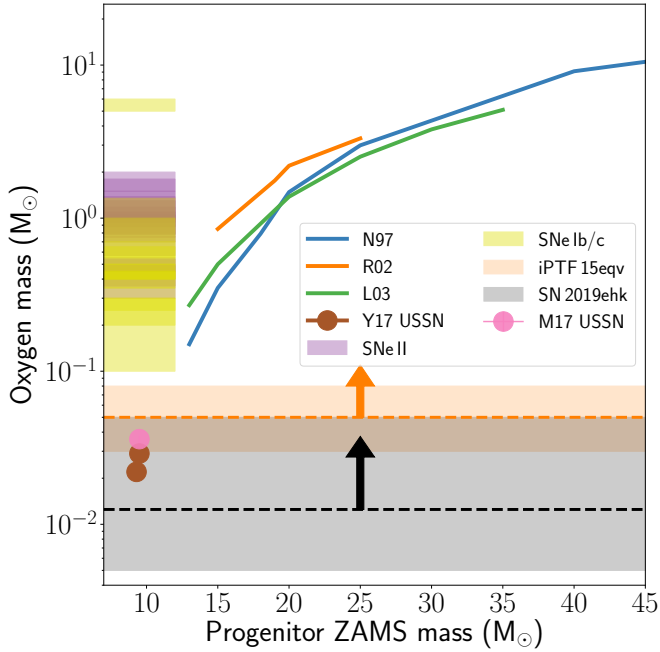


Figure 3. Comparison of the O mass lower limit estimate for SN 2019ehk (in shaded grey region) to models of synthesized O mass in core-collapse SNe as a function of the progenitor ZAMS mass. The blue, green and orange lines refer to nucleosynthesis models of Nomoto et al. (1997, N97), Rauscher et al. (2002, R02) and Limongi & Chieffi (2003, L03). We also plot O nucleosynthetic yields for models of low mass CO cores of ultra-stripped SNe (USSNe) from Moriya et al. (2017, M17) and Yoshida et al. (2017, Y17) scaled to the corresponding ZAMS mass expected from stellar evolution (Woosley & Heger 2015). For comparison, we plot estimated O masses for normal core-collapse SNe II and Ib/c on the left y-axis. We also show our estimated O mass for a late-time spectrum of another Ca-rich SN IIB iPTF 15eqv.

mass from Nomoto et al. (1997), Rauscher et al. (2002) and Limongi & Chieffi (2003). For comparison we show estimated O masses from a sample of core-collapse SNe of Type II and Type Ib/c from the compilation of Elmhamdi (2011), demonstrating that the O yields in most normal core-collapse SNe are consistent with $\approx 12 - 20 M_{\odot}$ progenitor ZAMS masses.

Specifically, Figure 3 demonstrates that the small O mass estimated for SN 2019ehk requires a much smaller progenitor ZAMS mass (and CO core mass) than the canonical models of core-collapse SNe that have been published for ZAMS masses of $\gtrsim 12 M_{\odot}$ (corresponding to CO core mass $\gtrsim 2.0 M_{\odot}$; Woosley & Heger 2015). We thus compare the O mass estimate to smaller CO core masses that have been simulated in the context of ultra-stripped SNe (Moriya et al. 2017; Yoshida et al. 2017). As shown in Figure 3, the synthesized O mass

estimates for these low mass CO cores are consistent with the range estimated for SN 2019ehk.

3.4. On the presence of hydrogen in the ejecta

SN 2019ehk was classified as a hydrogen-poor SN Ib in Jacobson-Galán et al. (2020) and Nakaoka et al. (2020), while De et al. (2020) reported the classification of this object as a Type IIB SN. In Figure 4, we plot peak-light optical spectra of SN 2019ehk together with a spectrum of the Type IIB SN 1993J (Matheson et al. 2000). We highlight the presence of absorption features in all the Balmer series transitions at velocities of 7500 km s^{-1} , and distinct He I transitions at 5000 km s^{-1} , consistent with compositionally stratified and homologous expanding ejecta for Type IIB SNe (Dessart et al. 2011). We note the similarities between SN 1993J and SN 2019ehk in the presence of all the Balmer absorption features as well as the flat-bottomed $H\alpha$ structure seen in other Type IIB SNe (Silverman et al. 2009; Marion et al. 2014).

The early time ‘flash’ spectra presented in Jacobson-Galán et al. (2020) also exhibit narrow but resolved emission lines of $H\alpha$ and He II (Figure 4). Such features are commonly seen in early time spectra of hydrogen-rich core-collapse SNe (Gal-Yam et al. 2014; Yaron et al. 2017). In the early nebular phase, SN 2019ehk exhibits nearly identical spectroscopic features as that of iPTF 15eqv (Figure 4), which was reported as a peculiar hydrogen-rich SN IIB which exhibited a nebular phase spectrum dominated by [Ca II] emission (Milisavljevic et al. 2017). We specifically note the presence of a broad emission feature near the $H\alpha$ transition, which led to the initial classification of iPTF 15eqv as a SN IIB since it was classified several weeks after peak light (Cao et al. 2015; Milisavljevic et al. 2017). At very late phases (> 200 days after peak), the spectra both SN 2019ehk and iPTF 15eqv are dominated by only [Ca II] emission, leading to their classification as ‘Ca-rich’ supernovae.

Hachinger et al. (2012) performed radiative transfer simulations for a range of stripped envelope SN progenitors with varying amounts of H and He left at the time of explosion (see their Figure 10). Specifically, they show that the flat-bottomed feature near $\approx 6400 \text{ \AA}$ as well as the weaker higher order Balmer series absorption features are commonly seen in their transitional Type IIB/Ib models, formed by absorption from the nearby $H\alpha$ and Si II $\lambda 6355$ transition. These transitional Type IIB/Ib models are achieved with small amounts of residual hydrogen in the progenitor, and suggest a remaining H mass of at least $M_H \approx 0.02 - 0.03 M_{\odot}$ in SN 2019ehk.

4. DISCUSSION

In this work, we have demonstrated that i) the late-time [OI] luminosity in SN 2019ehk is consistent with

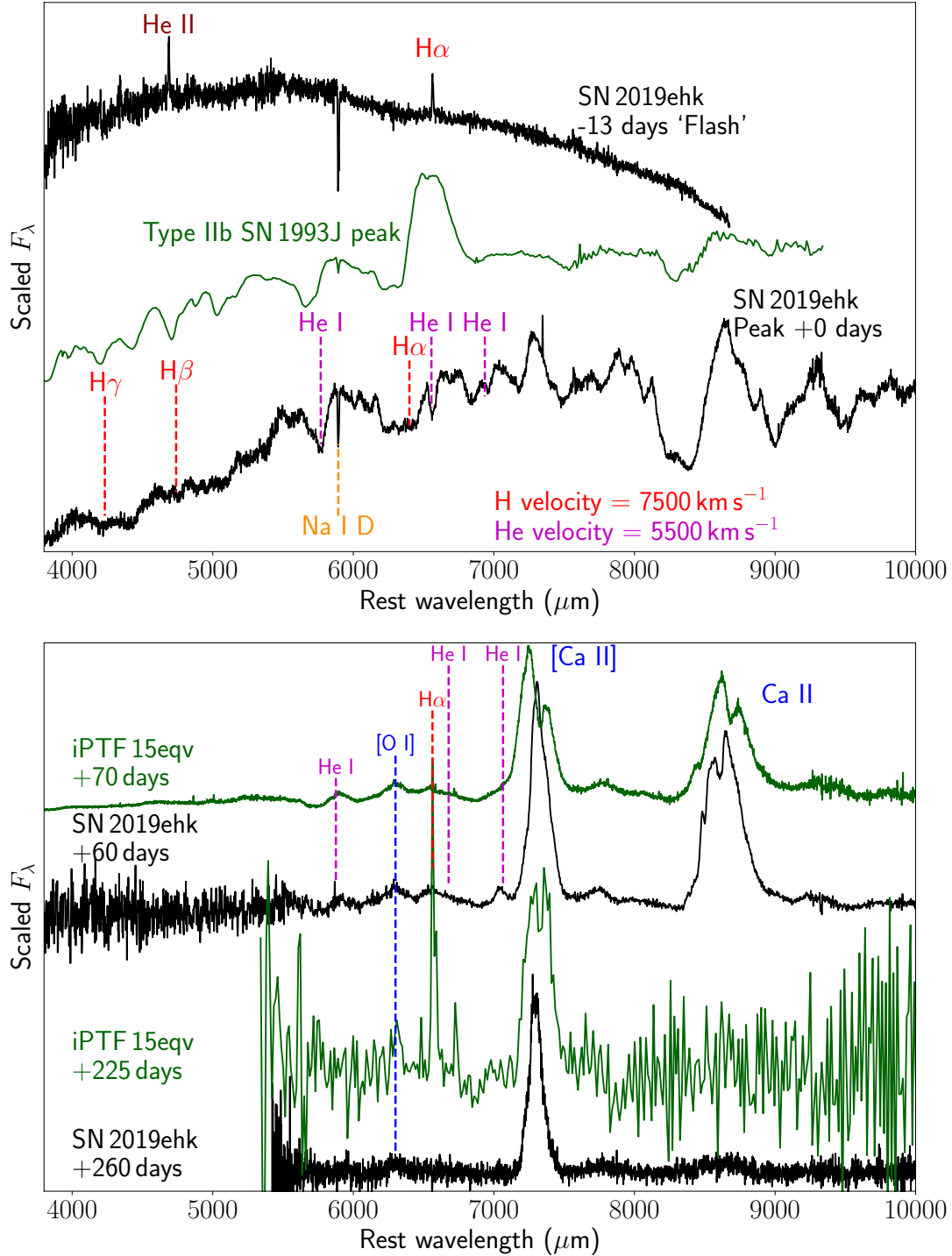


Figure 4. (Top panel) Spectra of SN 2019ehk around peak light. The very early spectrum at -13 days shows clear narrow emission lines of H α and He II, suggesting a ‘flash-ionized’ hydrogen-rich CSM. We show a comparison of our peak light spectrum of SN 2019ehk to that of the Type IIb SN 1993J, highlighting apparent absorption features of H at a velocity of 7500 km s^{-1} and He I at a velocity of 5500 km s^{-1} . The spectrum of SN 1993J has been artificially reddened with $E(B - V) = 0.75$ to match the continuum shape of SN 2019ehk for better visualization. Note the striking similarities between the two objects in the apparent Balmer and He I absorption features. (Bottom panel) Comparison of the early and late nebular phase spectra of SN 2019ehk and iPTF 15eqv (from Jacobson-Galán et al. 2020 and Milisavljevic et al. 2017), highlighting features of H, He I, [O I] and [Ca II].

very low O mass expected for low mass ($\approx 1.45\text{--}1.5 M_{\odot}$) CO cores of core-collapse SNe and ii) there is evidence for hydrogen in the early flash-ionized phase, photospheric phase and nebular phase spectra of SN 2019ehk – suggesting a classification as a Type IIb SN with at least $M_H \approx 0.03 M_{\odot}$ in and around the progenitor at the time of explosion.

In the case of the interpretation as a thermonuclear transient initiated by a He detonation during a white dwarf merger (Jacobson-Galán et al. 2020), it was suggested that the early time narrow H features were consistent with H-rich CSM (with hydrogen mass of $M_H \sim 10^{-4} M_{\odot}$) ejected at the time of merger. However, the presence of photospheric hydrogen suggests $M_H \gtrsim 0.02\text{--}0.03 M_{\odot}$, which is difficult to reconcile with this scenario since the progenitor CO + He binary white dwarfs are expected to be very deficient in hydrogen ($M_H \lesssim 10^{-4} M_{\odot}$; Podsiadlowski et al. 2003; Lawlor & MacDonald 2006; Zenati et al. 2019).

While Nakaoka et al. (2020) suggested that SN 2019ehk originated in an ultra-stripped core-collapse SN, hydrogen is not expected in the ejecta of ultra-stripped SNe with compact objects as close binary companions (Tauris et al. 2015). However, low mass progenitors of stripped core-collapse SNe can retain a large range of H and He masses depending on the nature of the companion and the initial binary period (Yoon et al. 2010; Zapartas et al. 2017; Laplace et al. 2020). The O mass estimate for SN 2019ehk suggests a ZAMS $\approx 9\text{--}9.5 M_{\odot}$ progenitor that forms a He core mass of $\approx 1.8\text{--}2.0 M_{\odot}$. Assuming a residual H mass of $\lesssim 0.1 M_{\odot}$, the inferred ejecta mass of SN 2019ehk of $\approx 0.5\text{--}0.6 M_{\odot}$ is consistent with a final CO core mass of $\approx 1.45\text{--}1.5 M_{\odot}$ that collapses to form a $\approx 1.3 M_{\odot}$ neutron star and ejects $\approx 0.5 M_{\odot}$ of material.

The evidence for dense nearby CSM as seen in the early time light curve and spectra (Jacobson-Galán et al. 2020) would then be explained by elevated mass loss prior to explosion as expected for low mass He cores (Woosley 2019; Laplace et al. 2020). Comparing our inferred parameters of SN 2019ehk to the single star models of Woosley & Heger (2015) and binary models of Laplace et al. (2020), who present detailed calculations of the late phase evolution of low mass He cores, we find that their solar metallicity models of progenitors between 9.0 and $9.5 M_{\odot}$ are strikingly similar to the estimated CO core mass and large pre-explosion radius (see Table A.2 in Laplace et al. (2020)). Finally, the low mass stripped core-collapse progenitor scenario is consistent with the $< 10 M_{\odot}$ star pre-explosion imaging constraints discussed in Jacobson-Galán et al. (2020).

The interpretation of the Ca-rich SN 2019ehk as a core-collapse SN adds another member to a growing class of core-collapse SNe that exhibit strong [Ca II] lines² – the others being the SN IIb iPTF 15eqv (Milisavljevic et al. 2017), SN Ic iPTF 14gqr (De et al. 2018b), and possibly the SN Ib iPTF 16hgs (De et al. 2018a), although iPTF 16hgs may also be consistent with a thermonuclear detonation. Kawabata et al. (2010) suggested that the SN Ib 2005cz could also have originated via this scenario, although its old environment argues against this interpretation (Perets et al. 2011). Some of the Ca-rich SNe reported in Filippenko et al. (2003) that were found in star forming galaxies may also be members of this class, although their poor photometric and spectroscopic coverage precludes a secure identification (Kasliwal et al. 2012).

iPTF 15eqv is perhaps the closest analog of SN 2019ehk, and was also shown to be a Type IIb core-collapse SN in a star forming environment (Milisavljevic et al. 2017) with a large [Ca II]/[O I] $\gtrsim 10$. For comparison, as in SN 2019ehk, we calibrate the latest nebular spectrum of iPTF 15eqv at ≈ 225 days with reported late-time photometry to derive the [O I] luminosity with [Ca II]/[O I] = 10 (Milisavljevic et al. 2017). We derive a [O I] luminosity of $\approx 1.2 \times 10^{38} \text{ erg s}^{-1}$, corresponding to a O mass of $\approx 0.03\text{--}0.08 M_{\odot}$ (shown in Figure 3). Using the estimated range of ^{56}Ni masses for this object, we also plot the normalized [O I] luminosity for this object in Figure 2. Both the [O I] luminosity and the O mass estimate for this object is consistent with a very low mass progenitor similar to SN 2019ehk.

Taking the large nebular [Ca II]/[O I] ratio and low [O I] luminosity as a signature of the low progenitor mass, the primary difference between SN 2019ehk and iPTF 15eqv would then be the final mass at the time of explosion. This leads to the different ejecta masses of $\approx 0.5 M_{\odot}$ in SN 2019ehk and $\approx 2\text{--}4 M_{\odot}$ in iPTF 15eqv (Milisavljevic et al. 2017), where iPTF 15eqv has a slightly more massive O core (higher [O I] luminosity) and H envelope (larger ejecta mass). Since stars in this low mass range ($\approx 9\text{--}9.5 M_{\odot}$) are still left with massive H envelopes of $\approx 7 M_{\odot}$ at the time of the SN (Woosley & Heger 2015) in single star evolution, the differences between the progenitors can be explained as differences in the binary stripping, which is a function of the nature and orbital period of the companion.

² In the case of the fast evolving ultra-stripped SN 2019dge (Yao et al. 2020), the late-time spectrum was dominated by CSM interaction with He-rich material, likely hiding the underlying nebular emission features from the ejecta

5. SUMMARY

We have presented very late-time imaging of the peculiar Ca-rich SN 2019ehk with the Keck-I telescope, which we use to perform accurate flux calibration of a contemporaneous late-time spectrum, and derive fluxes for the two most prominent nebular phase lines of [O I] and [Ca II]. In addition, we presented a high signal-to-noise peak light optical spectrum of the source, which we use to constrain the ejecta composition. To summarize our findings,

- The low [O I] luminosity in the nebular spectrum of SN 2019ehk suggests a very low O mass of $\approx 0.005 - 0.05 M_{\odot}$ (over the range of extinction and temperature assumptions). The inferred value is at least one order of magnitude smaller than that inferred for typical SNe II and SNe Ib/c.
- Comparing the inferred O mass to models of core-collapse SNe, we find consistency with the O yields expected from low CO cores of $\approx 1.45 - 1.5 M_{\odot}$, corresponding to He core masses of $\approx 1.8 - 2.0 M_{\odot}$ and ZAMS masses in the range of $\approx 9.0 - 9.5 M_{\odot}$, as derived from models of massive stars in both single and binary systems.
- We highlight the presence of Balmer series features in the peak light and early nebular phase spectra of SN 2019ehk, as well as the striking similarity of the $H\alpha$ profile shape to previous observations and radiative transfer models of SNe IIb. In addition, the H-rich CSM inferred from very early photometry and spectroscopy is similar to that observed in several young Type II core-collapse SNe. We thus suggest the classification of SN 2019ehk as a SN IIb.
- We find that the presence of photospheric hydrogen features (suggesting $M_H \gtrsim 0.02 - 0.03 M_{\odot}$) is inconsistent with models involving the thermonuclear detonation of a He shell during a white dwarf merger, as they are expected to retain only $M_H \sim 10^{-4} M_{\odot}$.
- We thus favor the interpretation of SN 2019ehk as a core-collapse supernova from a low mass $\approx 9.5 M_{\odot}$ progenitor, which has been stripped of most of its hydrogen envelope by a binary companion.

Our results provide evidence for a class of Ca-rich core-collapse SNe (including SN 2019ehk and iPTF 15eqv)

from low mass CO cores that form a distinct population from the thermonuclear Ca-rich gap transients found in old environments. While it is currently not obvious what photometric and spectroscopic properties distinguish this class from the old thermonuclear Ca-rich transients (apart from their star forming host environments), the presence of hydrogen in the ejecta of some objects (as demonstrated by peak light spectra of iPTF 15eqv and SN 2019ehk) provides strong evidence for the massive star scenario where the progenitors can retain a substantial amount of hydrogen ($M_H \gtrsim 0.01 M_{\odot}$) at the time of explosion. Detailed nebular phase modeling of the nucleosynthetic products generated from core-collapse explosions of low mass CO cores, which have not been presented in the literature till this date, hold the potential to reveal significant insights into this phenomenon.

ACKNOWLEDGMENTS

We thank W. Jacobson-Galan for providing the spectral sequence of SN 2019ehk. We thank J. Sollerman for constructive comments on this manuscript. We thank L. Bildsten and A. Polin for valuable discussions. We thank D. Perley for assistance with `lpipe`.

This work was supported by the GROWTH (Global Relay of Observatories Watching Transients Happen) project funded by the National Science Foundation under PIRE Grant No 1545949. Some of the data presented herein were obtained at the W.M. Keck Observatory, which is operated as a scientific partnership among the California Institute of Technology, the University of California and the National Aeronautics and Space Administration. The Observatory was made possible by the generous financial support of the W.M. Keck Foundation. The authors wish to recognize and acknowledge the very significant cultural role and reverence that the summit of Mauna Kea has always had within the indigenous Hawaiian community. We are most fortunate to have the opportunity to conduct observations from this mountain. AGY's research is supported by the EU via ERC grant No. 725161, the ISF GW excellence center, an IMOS space infrastructure grant and BSF/Transformative and GIF grants, as well as The Benoziyo Endowment Fund for the Advancement of Science, the Deloro Institute for Advanced Research in Space and Optics, The Veronika A. Rabl Physics Discretionary Fund, Paul and Tina Gardner, Yeda-Sela and the WIS-CIT joint research grant; AGY is the recipient of the Helen and Martin Kimmel Award for Innovative Investigation.

REFERENCES

- Becker, A. 2015, HOTPANTS: High Order Transform of PSF AND Template Subtraction.
<http://ascl.net/1504.004>
- Bellm, E. C., & Sesar, B. 2016, pyraf-dbsp: Reduction pipeline for the Palomar Double Beam Spectrograph.
<http://ascl.net/1602.002>
- Cao, Y., Kulkarni, S. R., Cook, D., & Vreeswijk, P. 2015, The Astronomer's Telegram, 8428, 1
- Cardelli, J. A., Clayton, G. C., & Mathis, J. S. 1989, ApJ, 345, 245, doi: [10.1086/167900](https://doi.org/10.1086/167900)
- De, K., Kasliwal, M. M., Cantwell, T., et al. 2018a, ApJ, 866, 72, doi: [10.3847/1538-4357/aadf8e](https://doi.org/10.3847/1538-4357/aadf8e)
- De, K., Kasliwal, M. M., Ofek, E. O., et al. 2018b, Science, 362, 201, doi: [10.1126/science.aas8693](https://doi.org/10.1126/science.aas8693)
- De, K., Kasliwal, M. M., Tzanidakis, A., et al. 2020, arXiv e-prints, arXiv:2004.09029.
<https://arxiv.org/abs/2004.09029>
- Dessart, L., & Hillier, D. J. 2015, MNRAS, 447, 1370, doi: [10.1093/mnras/stu2520](https://doi.org/10.1093/mnras/stu2520)
- . 2020, arXiv e-prints, arXiv:2007.02243.
<https://arxiv.org/abs/2007.02243>
- Dessart, L., Hillier, D. J., Livne, E., et al. 2011, MNRAS, 414, 2985, doi: [10.1111/j.1365-2966.2011.18598.x](https://doi.org/10.1111/j.1365-2966.2011.18598.x)
- Elmhamdi, A. 2011, AcA, 61, 179.
<https://arxiv.org/abs/1109.2318>
- Fang, Q., Maeda, K., Kuncarayakti, H., Sun, F., & Gal-Yam, A. 2019, Nature Astronomy, 3, 434, doi: [10.1038/s41550-019-0710-6](https://doi.org/10.1038/s41550-019-0710-6)
- Filippenko, A. V., Chornock, R., Swift, B., et al. 2003, IAUC, 8159
- Folatelli, G., Phillips, M. M., Burns, C. R., et al. 2010, AJ, 139, 120, doi: [10.1088/0004-6256/139/1/120](https://doi.org/10.1088/0004-6256/139/1/120)
- Fransson, C., & Chevalier, R. A. 1989, ApJ, 343, 323, doi: [10.1086/167707](https://doi.org/10.1086/167707)
- Frohmaier, C., Sullivan, M., Maguire, K., & Nugent, P. 2018, ApJ, 858, 50, doi: [10.3847/1538-4357/aabc0b](https://doi.org/10.3847/1538-4357/aabc0b)
- Frohmaier, C., Sullivan, M., Nugent, P. E., et al. 2019, MNRAS, 486, 2308, doi: [10.1093/mnras/stz807](https://doi.org/10.1093/mnras/stz807)
- Gal-Yam, A. 2017, Observational and Physical Classification of Supernovae (Cham: Springer International Publishing), 1–43, doi: [10.1007/978-3-319-20794-0_35-1](https://doi.org/10.1007/978-3-319-20794-0_35-1)
- Gal-Yam, A., Arcavi, I., Ofek, E. O., et al. 2014, Nature, 509, 471, doi: [10.1038/nature13304](https://doi.org/10.1038/nature13304)
- Grzegorzec, J. 2019, Transient Name Server Discovery Report, 2019-666, 1
- Hachinger, S., Mazzali, P. A., Taubenberger, S., et al. 2012, MNRAS, 422, 70, doi: [10.1111/j.1365-2966.2012.20464.x](https://doi.org/10.1111/j.1365-2966.2012.20464.x)
- Houck, J. C., & Fransson, C. 1996, ApJ, 456, 811, doi: [10.1086/176699](https://doi.org/10.1086/176699)
- Jacobson-Galán, W. V., Margutti, R., Kilpatrick, C. D., et al. 2020, arXiv e-prints, arXiv:2005.01782.
<https://arxiv.org/abs/2005.01782>
- Jerkstrand, A., Ergon, M., Smartt, S. J., et al. 2015, A&A, 573, A12, doi: [10.1051/0004-6361/201423983](https://doi.org/10.1051/0004-6361/201423983)
- Jerkstrand, A., Smartt, S. J., Fraser, M., et al. 2014, MNRAS, 439, 3694, doi: [10.1093/mnras/stu221](https://doi.org/10.1093/mnras/stu221)
- Kasliwal, M. M., Kulkarni, S. R., Gal-Yam, A., et al. 2012, ApJ, 755, 161, doi: [10.1088/0004-637X/755/2/161](https://doi.org/10.1088/0004-637X/755/2/161)
- Kawabata, K. S., Maeda, K., Nomoto, K., et al. 2010, Nature, 465, 326, doi: [10.1038/nature09055](https://doi.org/10.1038/nature09055)
- Laplace, E., Götberg, Y., de Mink, S. E., Justham, S., & Farmer, R. 2020, A&A, 637, A6, doi: [10.1051/0004-6361/201937300](https://doi.org/10.1051/0004-6361/201937300)
- Lawlor, T. M., & MacDonald, J. 2006, MNRAS, 371, 263, doi: [10.1111/j.1365-2966.2006.10641.x](https://doi.org/10.1111/j.1365-2966.2006.10641.x)
- Limongi, M., & Chieffi, A. 2003, ApJ, 592, 404, doi: [10.1086/375703](https://doi.org/10.1086/375703)
- Lunnan, R., Kasliwal, M. M., Cao, Y., et al. 2017, ApJ, 836, 60, doi: [10.3847/1538-4357/836/1/60](https://doi.org/10.3847/1538-4357/836/1/60)
- Marion, G. H., Vinko, J., Kirshner, R. P., et al. 2014, ApJ, 781, 69, doi: [10.1088/0004-637X/781/2/69](https://doi.org/10.1088/0004-637X/781/2/69)
- Matheson, T., Filippenko, A. V., Barth, A. J., et al. 2000, AJ, 120, 1487, doi: [10.1086/301518](https://doi.org/10.1086/301518)
- Milisavljevic, D., Patnaude, D. J., Raymond, J. C., et al. 2017, ApJ, 846, 50, doi: [10.3847/1538-4357/aa7d9f](https://doi.org/10.3847/1538-4357/aa7d9f)
- Moriya, T. J., Mazzali, P. A., Tominaga, N., et al. 2017, MNRAS, 466, 2085, doi: [10.1093/mnras/stw3225](https://doi.org/10.1093/mnras/stw3225)
- Mulchaey, J. S., Kasliwal, M. M., & Kollmeier, J. A. 2014, ApJL, 780, L34, doi: [10.1088/2041-8205/780/2/L34](https://doi.org/10.1088/2041-8205/780/2/L34)
- Nakaoka, T., Maeda, K., Yamanaka, M., et al. 2020, arXiv e-prints, arXiv:2005.02992.
<https://arxiv.org/abs/2005.02992>
- Nomoto, K., Hashimoto, M., Tsujimoto, T., et al. 1997, NuPhA, 616, 79, doi: [10.1016/S0375-9474\(97\)00076-6](https://doi.org/10.1016/S0375-9474(97)00076-6)
- Oke, J. B., & Gunn, J. E. 1982, PASP, 94, 586, doi: [10.1086/131027](https://doi.org/10.1086/131027)
- Oke, J. B., Cohen, J. G., Carr, M., et al. 1995, PASP, 107, 375, doi: [10.1086/133562](https://doi.org/10.1086/133562)
- Perets, H. B., Gal-yam, A., Crockett, R. M., et al. 2011, ApJL, 728, L36, doi: [10.1088/2041-8205/728/2/L36](https://doi.org/10.1088/2041-8205/728/2/L36)
- Perets, H. B., Gal-Yam, A., Mazzali, P. A., et al. 2010, Nature, 465, 322, doi: [10.1038/nature09056](https://doi.org/10.1038/nature09056)
- Perley, D. A. 2019, PASP, 131, 084503, doi: [10.1088/1538-3873/ab215d](https://doi.org/10.1088/1538-3873/ab215d)
- Podsiadlowski, P., Han, Z., & Rappaport, S. 2003, MNRAS, 340, 1214, doi: [10.1046/j.1365-8711.2003.06380.x](https://doi.org/10.1046/j.1365-8711.2003.06380.x)

- Podsiadlowski, P., Joss, P. C., & Hsu, J. J. L. 1992, *ApJ*, 391, 246, doi: [10.1086/171341](https://doi.org/10.1086/171341)
- Polin, A., Nugent, P., & Kasen, D. 2019, arXiv e-prints, arXiv:1910.12434. <https://arxiv.org/abs/1910.12434>
- Poznanski, D., Prochaska, J. X., & Bloom, J. S. 2012, *MNRAS*, 426, 1465, doi: [10.1111/j.1365-2966.2012.21796.x](https://doi.org/10.1111/j.1365-2966.2012.21796.x)
- Rauscher, T., Heger, A., Hoffman, R. D., & Woosley, S. E. 2002, *ApJ*, 576, 323, doi: [10.1086/341728](https://doi.org/10.1086/341728)
- Silverman, J. M., Mazzali, P., Chornock, R., et al. 2009, *PASP*, 121, 689, doi: [10.1086/603653](https://doi.org/10.1086/603653)
- Sollerman, J., Leibundgut, B., & Spyromilio, J. 1998, *A&A*, 337, 207
- Tauris, T. M., Langer, N., Moriya, T. J., et al. 2013, *ApJL*, 778, L23, doi: [10.1088/2041-8205/778/2/L23](https://doi.org/10.1088/2041-8205/778/2/L23)
- Tauris, T. M., Langer, N., & Podsiadlowski, P. 2015, *MNRAS*, 451, 2123, doi: [10.1093/mnras/stv990](https://doi.org/10.1093/mnras/stv990)
- Uomoto, A. 1986, *ApJL*, 310, L35, doi: [10.1086/184777](https://doi.org/10.1086/184777)
- Valenti, S., Yuan, F., Taubenberger, S., et al. 2014, *MNRAS*, 437, 1519, doi: [10.1093/mnras/stt1983](https://doi.org/10.1093/mnras/stt1983)
- Waldman, R., Sauer, D., Livne, E., et al. 2011, *ApJ*, 738, 21, doi: [10.1088/0004-637X/738/1/21](https://doi.org/10.1088/0004-637X/738/1/21)
- Woosley, S. E. 2019, *ApJ*, 878, 49, doi: [10.3847/1538-4357/ab1b41](https://doi.org/10.3847/1538-4357/ab1b41)
- Woosley, S. E., & Heger, A. 2007, *PhR*, 442, 269, doi: [10.1016/j.physrep.2007.02.009](https://doi.org/10.1016/j.physrep.2007.02.009)
- . 2015, *ApJ*, 810, 34, doi: [10.1088/0004-637X/810/1/34](https://doi.org/10.1088/0004-637X/810/1/34)
- Yao, Y., De, K., Kasliwal, M. M., et al. 2020, arXiv e-prints, arXiv:2005.12922. <https://arxiv.org/abs/2005.12922>
- Yaron, O., & Gal-Yam, A. 2012, *PASP*, 124, 668, doi: [10.1086/666656](https://doi.org/10.1086/666656)
- Yaron, O., Perley, D. A., Gal-Yam, A., et al. 2017, *Nature Physics*, 13, 510, doi: [10.1038/nphys4025](https://doi.org/10.1038/nphys4025)
- Yoon, S.-C., Woosley, S. E., & Langer, N. 2010, *ApJ*, 725, 940, doi: [10.1088/0004-637X/725/1/940](https://doi.org/10.1088/0004-637X/725/1/940)
- Yoshida, T., Suwa, Y., Umeda, H., Shibata, M., & Takahashi, K. 2017, *MNRAS*, 471, 4275, doi: [10.1093/mnras/stx1738](https://doi.org/10.1093/mnras/stx1738)
- Zapartas, E., de Mink, S. E., Izzard, R. G., et al. 2017, *A & A*, 601, A29, doi: [10.1051/0004-6361/201629685](https://doi.org/10.1051/0004-6361/201629685)
- Zenati, Y., Toonen, S., & Perets, H. B. 2019, *MNRAS*, 482, 1135, doi: [10.1093/mnras/sty2723](https://doi.org/10.1093/mnras/sty2723)